# EXCITATIONS OF PYRONIN Y AND PYRONIN B DYES IN AQUEOUS SOLUTION: COMPARATIVE THEORETICAL ANALYSIS

## Leontieva S.V.
Black Sea Higher Naval Orders of the Red Star School named after P.S. Nakhimov
*Dybenko st., 1a, Sevastopol, 299028, Russia; e-mail:tezidi@gmail.com*

**Abstract.** To elucidate the effect of side groups on the excitation of xanthene dyes, pyronin Y (PY) and pyronin B (PB) were studied by DFT/TD-DFT. The calculation results were compared with each other, as well as with the data for the acridine red dye previously studied. The O3LYP/6-31++G(d,p)/IEFPCM theory level reproduced well the experimental spectra of PY and PB aqueous solutions. According to calculations, the short-wavelength shoulders of these spectra are caused by vibronic transitions. The side groups significantly affect the set of vibronic transitions. The photoexcitation significantly changes the intensities of IR vibrations. The side groups of these xanthene dyes (aminodimethyl/aminodiethyl) strongly influence the vibrations of their chromophores. HOMOs cover the side groups of both dyes to a greater extent compared to LUMOs. The configurations of both frontier orbitals around the chromophores are identical for PY and PB. The dipole moment of the dye molecules in the excited state turned out to be greater than in the ground state. In the ground state, the dipole moment of the PB is 2.5 times greater than that of the PY, and in the excited states, it is 1.7 times less. The transition moments of PY and PB are almost identical to each other. Considering site-specific solute-solvent interactions in the form of an explicit assignment of water molecules that form strong hydrogen bonds with the dye cations was performed.

***Key words:** TD-DFT, vibronic transitions, aqueous solution, pyronin Y, pyronin B, absorption spectrum.*

## INTRODUCTION

Pyronin Y (PY, also known as pyronin G and pyronin J), and pyronin B (PB), are xanthene dyes [1]. PY is used for selective staining of RNA [2,3], as a fluorescent probe [4], as an optical sensor [5], and in solar cells [6,7]. PB is used for differential staining of nucleic acids only, in a mixture with methyl green [2]. One of the reasons for the limited use of PB compared to PY may be the bulkiness of the molecule of this dye, due to the presence of branched diethylamino groups (Fig. 1).

Using optical methods, it was found that, in addition to non-covalent binding to nucleic acids [2,3,8-10], PY and PB are also capable of forming non-covalent complexes with proteins [11], glucose [5], cyclodextrins [12], as well as with clay [13], nanoparticles [14,15] and nanocomposites [16]. Spectrophotometry has also been applied to study PY [10,12,17-24] and PB [12,18,24] aggregations and heteroassociation [25]. The optical properties of the dyes have also been studied experimentally in sufficient detail, both in films [26] and in various solvents [27-33]. However, a theoretical study of the electronically excited states of PY and PB was carried out only in three works [34-36]. Authors of these papers performed a systematic study of the vertical electronic transitions of these two xanthenes and large sets of rhodamine dyes using quantum chemistry methods (time-dependent density functional theory (TD-DFT) [34-36], algebraic-diagrammatic construction through second-order ADC(2), Extended Multi-Configuration Quasi-Degenerate Perturbation Theory (XMC-QDPT2) [35], and coupled-cluster CC2 [36]) with implicit water assignment [34,35] using the CPCM [37] model and in a gas phase [36]. It turned out that, in general, the TD-DFT and CC2 give the values of the transition energies overestimated in comparison with the experiment, and ADC(2) and XMC-QDPT2 – underestimated ones. In particular, for PY and PB, the best agreements with experiment ($E_{max}$=2.27 eV and 2.24 eV, respectively, in aqueous solution) were achieved using TD-DFT/BP86/6-31+G(d,p)/CPCM ($E_{vert}$=2.42 eV and 2.38 eV, respectively) and XMC-QDPT2 ($E_{vert}$=2.27 eV and 2.16 eV, respectively) theory levels [35]. There is an excellent agreement between the theoretical result and the experiment in the latter case! In Ref. [34], at the B3LYP/6-31+G(d,p)/CPCM theory level, the
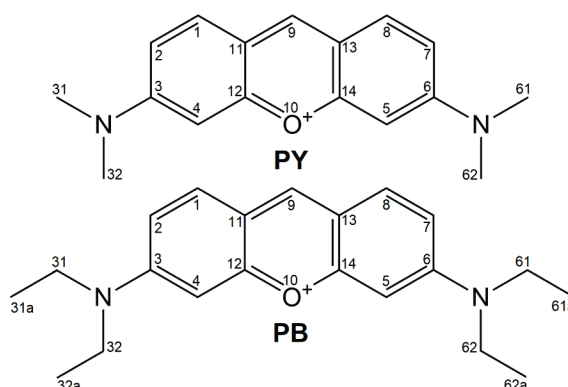


**Figure 1**. Chemical structures of PY and PB cations

$E_{vert}$=2.64 eV and 2.61 eV values were obtained for the PY and PB, respectively, in aqueous media. For PY in the gas phase [36], $E_{vert}$=2.98 eV (TDDFT) and $E_{vert}$=2.58 eV (CC2) values were obtained vs. the experimental $E_{max}$=2.40 eV. However, the vertical transition model is quite simplified, although it is widespread in the literature (see review [38]). It does not consider the vibronic transitions, and therefore does not allow theoretically reproducing the asymmetric form of the experimental absorption and emission spectra of organic molecules. At the same time, the shape of the spectrum reflects the pattern of the excited states of the molecule and the transitions between them [39]. Thus, the absorption spectra of PY and PB both in an aqueous solution [2,10,23,24,33] and in non-aqueous solvents [2,28,31] contain a short-wavelength shoulders. Some authors [33] traditionally consider them to be dimeric. However, these shoulders are observed in the spectra of highly diluted ($10^{-7}$ M) PY and PB solutions [15], in which the dimers contents, according to estimation from Ref. [32], are negligible. In addition, the short-wavelength shoulder is also contained in the spectrophotometrically resolved spectra of the PY and PB monomers [10,15,17,18]. The authors of Ref. [15] believe that the shoulders are of vibronic origin. Also, the shoulders can be due to separate electronic transitions. To answer this question, we calculated the vibronic absorption spectra of PY and PB in the visible region of the spectrum and analyzed their excited states and their interaction with the solvent. We also performed a comparative analysis of the excitations of these dyes to determine the effect of their side groups on them (see Fig. 1). Previously, a similar study [40] was performed by us for another xanthene dye, acridine red (AR), with side aminomethyl groups.

## METHODS

The initial spatial structures of the PY and PB cations were taken from the PubChem database (CIDs 7085 and 16524, respectively). These initial structures were then optimized at the O3LYP/6-31++G(d,p) theory level in both the ground and excited states. This theory level was chosen as optimal in our previous study of the related xanthene compound acridine red [40]. There were no imaginary frequencies in the IR spectra of these optimized structures, which indicated that the global minima of the PES had been reached (see Fig. 2) and made it possible to calculate the vibronic spectra.

The ground and excited states of the dyes were calculated using DFT and TD-DFT, respectively. In this case, the adiabatic Hessian and the harmonic approximation were used. Anharmonic effects should be small for rigid and semirigid molecules [41], such as the studied phenanthridines. Verification of the theory levels was carried out by comparing the calculated vibronic absorption spectra with the experimental ones, both in terms of the position of the maxima ($\lambda_{vibron}$ vs. $\lambda_{max}$) and shapes.

The vibronic absorption spectra of PY and PB in an aqueous solution were calculated using the time-independent DFT methodology [42] implemented in the Gaussian16 software package [43]. According to the Franck-Condon principle [44], the electronic transition occurs at fixed $R_{GS}$ positions of the nuclei corresponding to the ground state, i.e. is vertical in Fig. 2 (yellow arrow). Correspondingly, the electric dipole moment also does not change during the transition. The application of the Franck-Condon principle to the analysis of absorption and emission of organic molecules is described in detail in Ref [41].

The nonequilibrium state of a molecule with an excited electron shell and a nuclear core that retains the same configuration as in the ground state will be denoted as Franck-Condon (FC) point. This non-equilibrium of the nuclear core with respect to electrons activates its vibrational energy levels (green wave in Fig. 2). Thus, the transition is not purely electronic, but vibronic. Therefore, in this work, in addition to the vibronic absorption spectra, we also analyzed the calculated IR spectra of both dye states. The probability of a vibronic transition depends on the sets of vibrational states of the ground and excited electronic states. Since the molecule under consideration is in solution, the polarization of the solvent closest to it is also nonequilibrium, and in this work, it is described using the state-specific polarizable continuum model [45]. Then the nuclei of the dissolved molecule are displaced, adjusting to the excited electron shell. The solvent also relaxes (its reaction field is described by the equilibrium solvation model [46]), and the "solute molecule+solvent" system passes (red arrow in
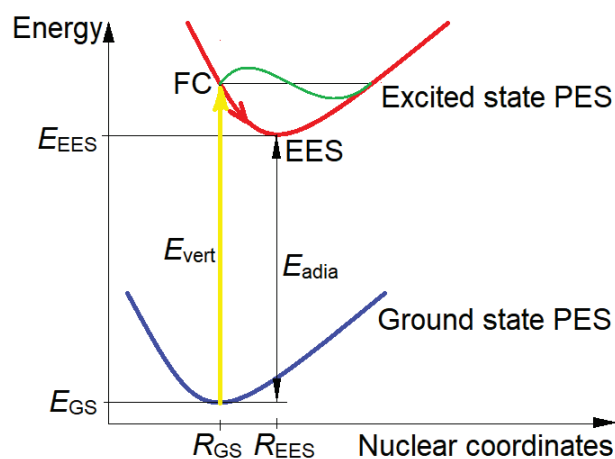


**Figure 2**. Simplified excitation diagram

Fig. 2) into an excited equilibrium state (EES). The difference between the energies of the ground and excited equilibrium states is usually called the adiabatic energy, $E_{adia}=E_{EES}-E_{GS}$ (see Fig. 2).

The broadening of the vibronic bands was carried out using Gaussians with half-width at half-maximum HWHM=600 cm$^{-1}$, and for IR peaks HWHM=4 cm$^{-1}$ was used. The simulated temperature was assumed to be T=298 K. The electron density distribution was quantitatively described using NPA charges [47]. The calculated spectra, as well as the visualization of the calculated structures of dyes, MOs, distributions of electron densities, and electrostatic potentials, were performed using the Gaussview6.0 software package [48].

### RESULTS AND DISCUSSION

The vibronic absorption spectra obtained using the O3LYP/6-31++G(d,p)/IEPCM theory level are in excellent agreements with the experiments ($\lambda_{max}$=546 nm, $E_{max}$=2.27 eV [8,15,16,27,30,33]) for PY and $\lambda_{max}$=552…554 nm, $E_{max}$≈2.24 eV [15,25,27,33] for PB) on the positions of the main maxima ($\lambda_{vibron}$=545 nm, $E_{vibron}$=2.28 eV for PY and $\lambda_{vibron}$=554 nm, $E_{vibron}$=2.24 eV for PB). At the same time, the shoulders in the calculated spectra ($\lambda_{shoulder}$≈512 nm for PY and ≈520 for PB), although their positions are in good agreement with the experimental ones, are lower (Fig. 3). The shoulders of the experimental spectra are due to the sum of the contributions of vibronic transitions and dimer absorption. This feature also took place for AR [40]. How can you see the shoulders in the absorption spectra has a vibronic origin (see Fig. 3). These vibronic transitions involve compression-stretching vibrations of chromophore rings. The side groups significantly affect the set of vibronic transitions (see Table 1).

Comparing the calculated IR spectra of PY and PB in the ground and excited states (Figs. 4 and 5), one can see that photoexcitation significantly changes the intensities of vibrations. For PY, vibrations #54, #58 and #68 are amplified, and vibrations #60, #68 and #90 are weakened (see Fig. 4). For PB, vibrations #66 and #81 are amplified, and vibration #108 is weakened (see Fig. 4). All these vibrations are compression-stretching or shears of the chromophores. In this case, the photoinduced decrease in the frequencies of these vibrations is small ($\Delta v$≈-50 cm$^{-1}$). A comparison between the calculated IR spectra for PY and PB shows significant differences between them. Thus, the side groups of these xanthene dyes (aminodimethyl/aminodiethyl) strongly influence the vibrations of their chromophores. The calculated IR spectra of the ground and excited states of AR containing aminoethyl side groups [40] also differ essentially from the spectra of PY and PB.
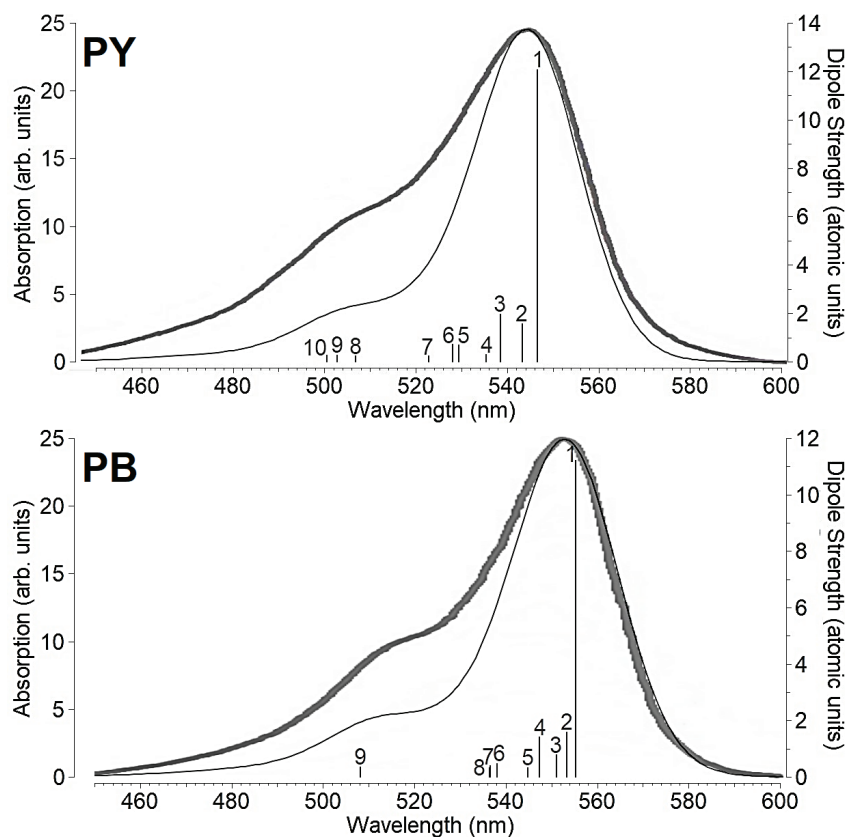


**Figure 3**. The calculated vibronic absorption spectra of PY and PB in aqueous solution (thin lines) and the corresponding experimental spectra (10$^{-7}$ M) from Ref. [15] (thick lines, permission from Elsevier, order 5115921255201). The vertical sticks are the dipole strength of the vibronic transitions from Table 1

**Table 1.** Calculated parameters of vibronic transitions during PY and PB photoexcitations in an aqueous solution

| # | Transition | $\lambda$ (nm) | E (eV) | $\nu$ ($cm^{-1}$) | I ($cm^{-1}$/ (molecule·$cm^{-2}$)) | p (atomic units) | Definition of vibrations |
|---|---|---|---|---|---|---|---|
| | | | | | PY | | |
| 1 | $0_0 \to 0^0$ | 548 | 2.26 | 0 | 181600 | 12.0 | - |
| 2 | $0_0 \to 6^1$ | 544 | 2.28 | 107 | 23650 | 1.56 | Flexural vibrations of a chromophore in its plane |
| 3 | $0_0 \to 15^1$ | 540 | 2.30 | 266 | 29880 | 1.95 | Compression-stretching of the chromophore along its long axis |
| 4 | $0_0 \to 6^1 15^1$ | 537 | 2.31 | 107+266 | 4217 | 0.27 | see above |
| 5 | $0_0 \to 28^1$ | 531 | 2.34 | 575 | 10540 | 0.68 | Compression-stretching of the central ring of the chromophore along its short axis |
| 6 | $0_0 \to 32^1$ | 529 | 2.34 | 627 | 10950 | 0.70 | |
| 7 | $0_0 \to 40^1$ | 524 | 2.36 | 811 | 3534 | 0.22 | Shear vibrations of the side rings of the chromophore |
| 8 | $0_0 \to 71^1$ | 509 | 2.44 | 1397 | 3755 | 0.23 | Compression-stretching of the side rings of the chromophore |
| 9 | $0_0 \to 90^1$ | 505 | 2.46 | 1552 | 4335 | 0.27 | Shear vibrations of all chromophore rings |
| 10 | $0_0 \to 92^1$ | 503 | 2.47 | 1639 | 4076 | 0.25 | Compression-stretching of all rings of the chromophore |
| | | | | | PB | | |
| 1 | $0_0 \to 0^0$ | 556 | 2.23 | 0 | 166400 | 11.2 | - |
| 2 | $0_0 \to 5^1$ | 554 | 2.24 | 61.3 | 23560 | 1.58 | Torsional vibration of diethylamino groups |
| 3 | $0_0 \to 11^1$ | 552 | 2.25 | 133 | 11670 | 0.780 | Flexural vibration of a chromophore in its plane |
| 4 | $0_0 \to 19^1$ | 548 | 2.26 | 253 | 21210 | 1.41 | Compression-stretching of the chromophore along its long axis |
| 5 | $0_0 \to 24^1$ | 546 | 2.27 | 334 | 4768 | 0.315 | Pendulum vibrations of terminal methyl groups perpendicular to the plane of the chromophore |
| 6 | $0_0 \to 36^1$ | 539 | 2.30 | 559 | 7017 | 0.458 | Compression-stretching of the central ring of the chromophore along its short axis |
| 7 | $0_0 \to 39^1$ | 538 | 2.31 | 613 | 6074 | 0.396 | Shear vibrations of the side rings of the chromophore |
| 8 | $0_0 \to 40^1$ | 538 | 2.31 | 615 | 4660 | 0.304 | |
| 9 | $0_0 \to 120^1$ | 510 | 2.43 | 1624 | 5675 | 0.351 | Compression-stretching of the side rings of the chromophore along its long axis |

$\lambda$ is the wavelength, E is the energy of the vibronic transition, $\nu$ is the vibration frequency, I is the line intensity, and p is the dipole strength
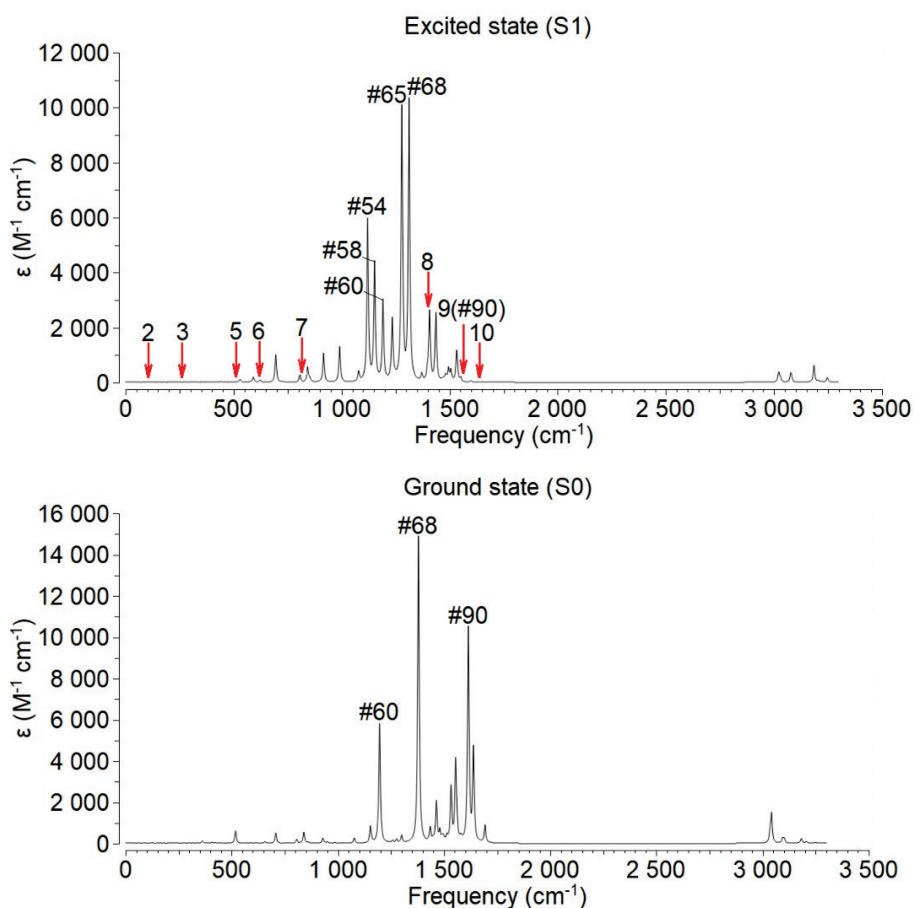
**Figure 4**. Calculated IR spectra of PY in aqueous solution. The peaks of the IR spectrum of the excited state, corresponding to the vibration frequencies involved in vibronic transitions (see Table 1), are shown by red arrows
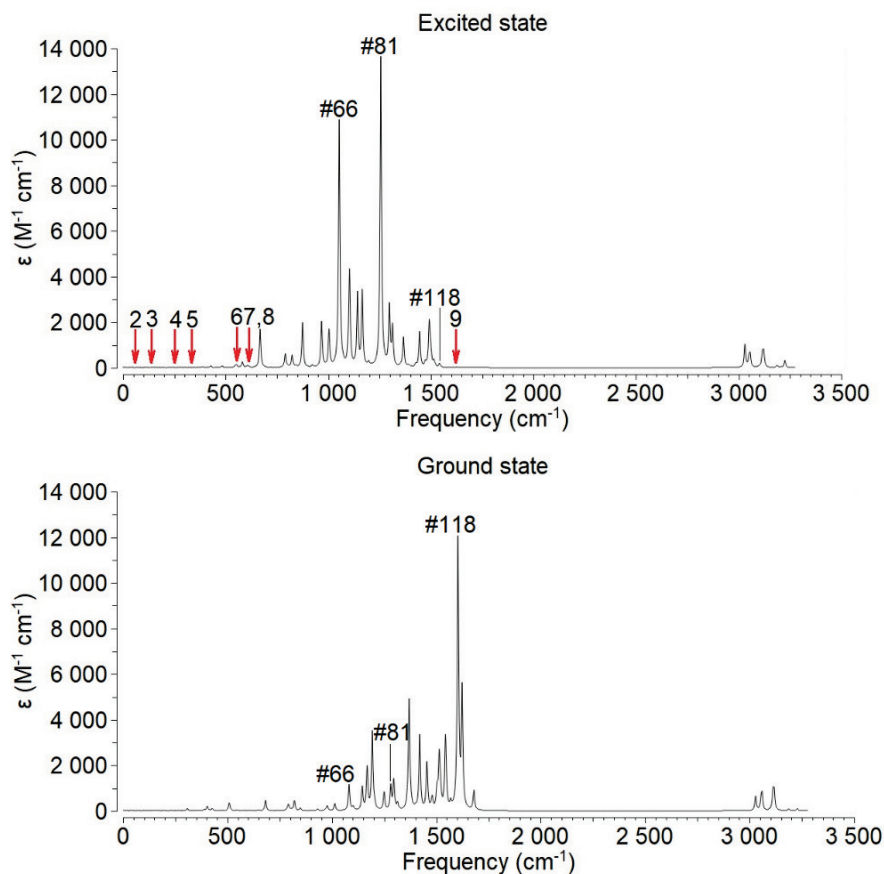


**Figure 5**. Calculated IR spectra of PB in an aqueous media

**Table 2.** Calculated parameters of ground and excited electronic states and transitions between them ($C_1$ point group of symmetry) in the visible and near UV regions of spectrum for PY in an aqueous solution

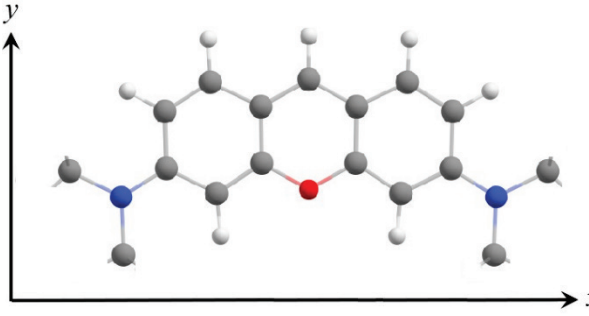| Electronic states | $E_{eq}$* (eV) | Electronic transition | $\lambda_{adia}$ (nm) | $E_{adia}$ (eV) | $\lambda_{vert}$ (nm) | $E_{vert}$ (eV) | $\lambda_{vibron}$ (nm) | $E_{vibron}$ (eV) | f | Involved transitions |
|---|---|---|---|---|---|---|---|---|---|---|
| | | | | | PY | | | | | |
| $S_0$ (GS) | -22963.24 | $S_0 \rightarrow S_1$ | 519 | 2.39 | 468 | 2.65 | 545 | 2.28 | 1.04 | HOMO→LUMO |
| $S_1$ (ES$_1$) | -22960.85 | | | | | | | | | |
| $S_2$ (ES$_2$) | -22960.31 | $S_0 \rightarrow S_2$ | 423 | 2.93 | 394 | 3.14 | 446 | 2.78 | 0.0033 | (HOMO-1)→LUMO |
| $S_3$ (ES$_3$) | -22959.62 | $S_0 \rightarrow S_3$ | 343 | 3.62 | 321 | 3.86 | 353 | 3.51 | 0.0439 | (HOMO-2)→LUMO |
| | | | | | PB | | | | | |
| $S_0$ (GS) | -27238.51 | $S_0 \rightarrow S_1$ | 532 | 2.33 | 482 | 2.57 | 554 | 2.24 | 1.08 | HOMO→LUMO |
| $S_1$ (ES$_1$) | -27236.18 | | | | | | | | | |
| $S_2$ (ES$_2$) | -27235.67 | $S_0 \rightarrow S_2$ | 437 | 2.84 | 407 | 3.05 | 452 | 2.74 | 0.0056 | (HOMO-1)→LUMO |
| $S_3$ (ES$_3$) | -27234.97 | $S_0 \rightarrow S_3$ | 350 | 3.54 | 330 | 3.76 | 361 | 3.43 | 0.0388 | (HOMO-2)→LUMO |

*equilibrium energy (PES minima, see Fig. 2)

According to calculations, the two next electronic transitions ($S_0 \rightarrow S_2$ and $S_0 \rightarrow S_3$) of PY and PB in the visible and near UV regions have very low f oscillator strength values (Table 2), and therefore do not make a significant contribution to the absorption spectra. When calculating the vibronic spectra of the $S_0 \rightarrow S_1$ transitions, the sums of the Franck-Condon factors were 99.94% for PY and 99.81 % for PB. Due to the larger number of atoms in PY compared to PB, the energies of its ground and excited states also turn out to be higher in absolute value. For AR, the modules of the corresponding quantities are even smaller [40].

The visualization of the frontier MOs involved in the $S_0 \rightarrow S_1$ electronic transitions considered is shown in Fig. 6. It should be noted that in this work they are visualized for the first time. As can be seen, HOMOs cover the side groups of both dyes to a greater extent compared to LUMOs. At the same time, the configurations of both frontier orbitals around the chromophores are identical for PY and PB. HOMOs do not include O10 heterocyclic oxygen atoms as well as most hydrogen atoms.

According to calculations, the dipole moments μ of the dye molecules increase upon photoexcitation: $\mu_{GS} < \mu_{FC} < \mu_{ES}$ (Table 3). This pattern corresponds to the $\pi \rightarrow \pi^*$ type of electronic transition and positive solvatochromism [57]. It is interesting to note that in the ground state the μ of the PB is 2.5 times greater than that of the PY, and in the excited states it is 1.7 times less. Due to the axial symmetry of the molecules of both dyes, the μ of their ground and excited states are directed across the chromophore - from the C9 atom to the O10 atom. An explanation of the photoinduced increase in μ based on the analysis of atomic charges will be given below. The transition moments M are directed along the dye chromophores and are almost identical to each other. The values of μ and M for PY and PB are calculated for the first time in this work: oddly enough, for these classical dyes, these data are not available in the literature. Note that for the AR, the corresponding calculated values were $\mu_{GS}$=0.955 D, $\mu_{FC}$=2.80 D, $\mu_{EES}$=2.79 D, and M=11.9 D [40].
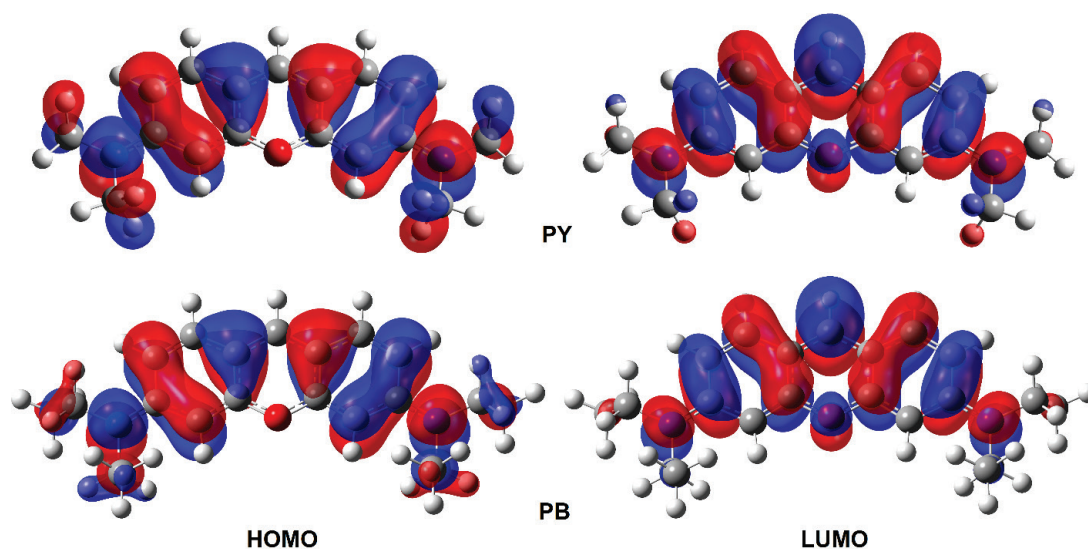


**Figure 6**. Frontier MOs, the transitions between which correspond to the main absorption peaks in the visible region. Positive lobes are shown in red and negative lobes in blue. Isovalue is 0.02 e/(a.u$^3$) and isodensity cutoff is 0.0004 e/(a.u$^3$)

**Table 3.** Calculated moments of PY and PB cations in an aqueous solution



The coordinate axes are directed along the principal axes of inertia of the molecules

| Dipole moment (D) | Ground state ($S_0$) | Excited state ($S_1$) | | Ground to excited state transition dipole moment (D) | |
|---|---|---|---|---|---|
| | | Franck-Condon (FC) | Equilibrium (ES) | | |
| PY | | | | | |
| $\mu_x$ | -0.0077 | -0.0082 | -0.0102 | $M_x$ | 12.0 |
| $\mu_y$ | -0.290 | -2.45 | -2.40 | $M_y$ | 0.0000 |
| $\mu_z$ | 0.0039 | 0.0040 | 0.0029 | $M_z$ | -0.0013 |
| $\mu$ | 0.290 | 2.45 | 2.40 | M | 12.0 |
| PB | | | | | |
| $\mu_x$ | 0.0048 | 0.0020 | -0.0008 | $M_x$ | 12.3 |
| $\mu_y$ | 0.707 | -1.45 | -1.37 | $M_y$ | 0.0000 |
| $\mu_z$ | -0.162 | 0.245 | 0.245 | $M_z$ | 0.0000 |
| $\mu$ | 0.725 | 1.47 | 1.39 | M | 12.3 |

However, PY and PB do not show pronounced solvatochromism: their absorption maxima are respectively $\lambda_{max}$=543 nm and 554 nm in dioxane ($E_T^N$=0.164, normalized empirical microscopic solvent polarity parameter [49]), 549 nm and 555 nm in tetrahydrofuran ($E_T^N$=0.207), 547 nm, and 553 nm in acetonitrile ($E_T^N$=0.460), 552 nm and 557 nm in dimethylformamide ($E_T^N$=0.386), 547 nm and 553 nm in ethanol ($E_T^N$=0.654), and 546 nm and 552 nm in water ($E_T^N$=1.000) [28]. Therefore, it can be expected that, in addition to dipole-dipole interactions with the solvent, site-specific interactions (hydrogen bonds) make a significant contribution. The latter will be discussed below.

To understand the photoinduced charge redistribution in the PY and PB molecules, we analyzed the NPA charges of heavy (non-hydrogen) atoms in the ground and excited states. The charges of the atoms of the chromophores of both dyes are close to each other, and the charges of the corresponding atoms of the side groups differ greatly, apparently due to their different structure. The GS→FC vertical transitions lead to a significant increase in electron density at the C9 atom and a decrease at C11 and C13 atoms (Fig. 7). The same picture took place earlier for AR [40]. For PY, this charge shift is larger compared to PB (see Fig. C4), which partly explains its higher absorption energy ($E_{max}$=2.27 eV for PY vs. 2.24 eV for PB, see above). Therefore, the $\mu_y$ increases in absolute value, and, in general, the $\mu$ increases (see Table 3). The FC→EES relaxations lead to weak changes in the atomic charges. In turn, this causes a slight decrease of $\mu_y$ modulus and an insignificant decrease in the $\mu$ of both cations. Visualizations of the differences in electron densities are shown in Fig. 8. It can be seen from them that the least involved in the photoinduced redistributions of electron densities are the hydrogen atoms of the methyl groups, as well as H2, H4, H5, and H7 atoms of the chromophore.
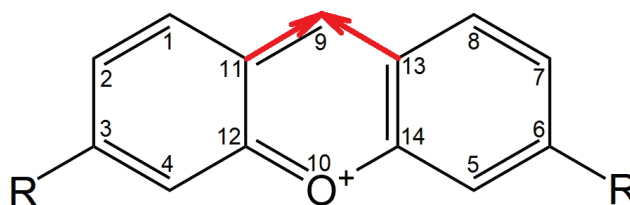


**Figure 7**. The main photoinduced shift of electron density in the chromophore of PY and PB
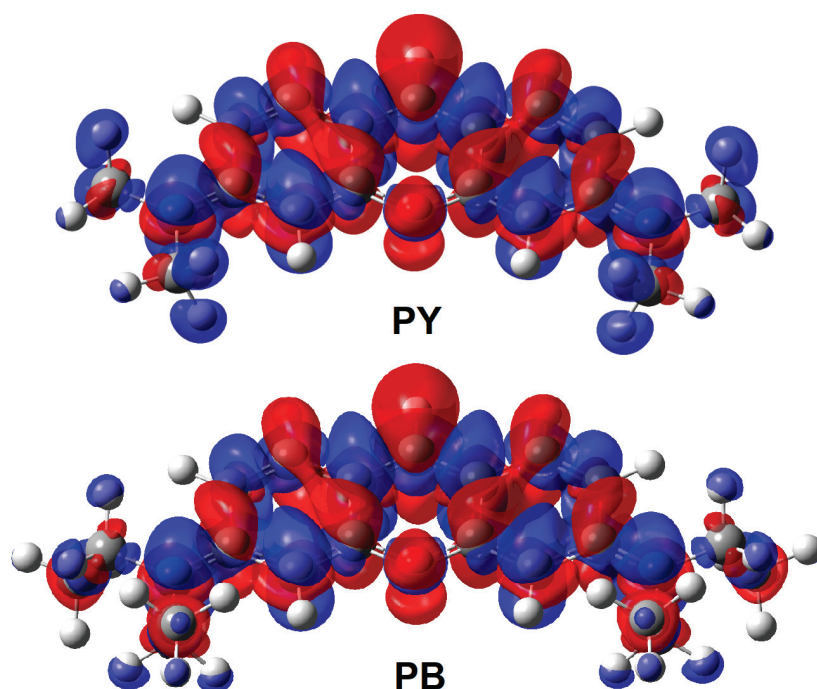
**Figure 8**. The electron density difference between Franck-Condon and ground states of PY and PB cations. Regions of positive values are shown in red and negative values in blue

Strong H-bonds between solute and solvent are site-specific interactions that are considered in the solvent continuum model used here averaged only. To estimate the effect of these H-bonds on the photoexcitation of the PY and PB molecules, an attempt was made to calculate the vibronic absorption spectra for the "PY+$H_2O$" and "PB+$H_2O$" hydrated complexes (Fig. 9).

According to calculations, the hydrogen bonds of PY and PB with water molecules in the excited state are stronger than in the ground state, which is manifested in their shortening (see Fig. 9). The phenomenon of enhanced hydrogen bonds with a solvent upon photoexcitation of various organic molecules was first discovered [50] and studied in detail [51] by Zhao and Han. The vibronic absorption spectrum of the "PY+$H_2O$" compared with a single PY cation has an artifact short-wavelength maximum at $\lambda_{vibron2}$=448 nm which is not observed in the experiment, and its absorption maximum is at $\lambda_{vibron}$=548 nm, i.e. the spectrum is redshifted by ≈3 nm. The absorption intensity decreases slightly (cf. Figs. 4 and 10). The number of vibronic transitions has reduced from 10 to 9, and the transitions themselves have changed significantly (cf. Figs. 4 and 10, Table 1).
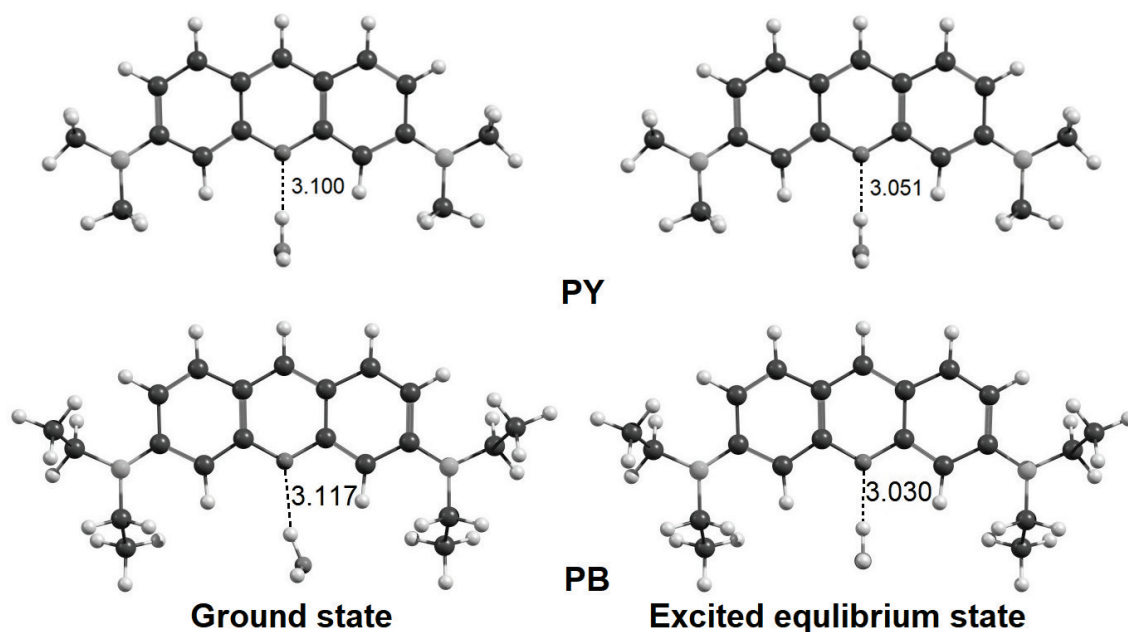


**Figure 9**. Calculated structures of the PY and PB hydration complexes with water molecules. Strong hydrogen bonds with their lengths in Å are shown with dotted lines
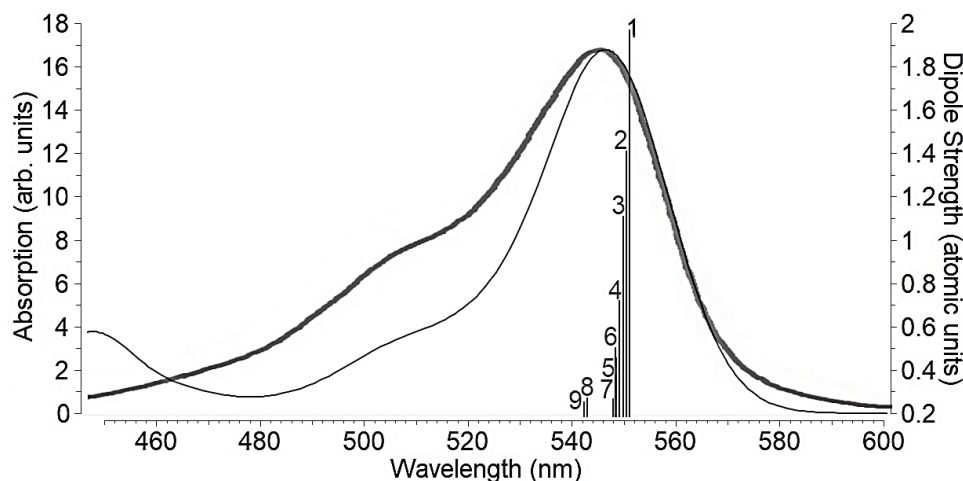
**Figure 10**. The calculated vibronic absorption spectrum of the "PY+H₂O" system (thin line) and the experimental spectrum ($10^{-7}$ M PY in water) from Ref. [15] (thick line)

For the "PB+H₂O" system, in the ground state, the bound water molecule is in the plane of the chromophore, while in the EES due to steric hindrances from the hydrogen atoms H4 and H5, it shifts, leaving it closer to us (see Fig. 9). The difference in the structures of the hydrating complex in the GS and EES turned out to be so significant that this led to a failure in the procedure of vibronic spectrum calculation.

For both dyes, the addition of strongly bound water molecules has little effect on their IR spectra (cf. Fig. 4 and 5). Visually, these differences are manifested in the fact that the most high-frequency ($\sim$4000 cm$^{-1}$) vibrations of hydrogen atoms of water molecules are added. The configurations of the frontier orbitals of the "PY+H₂O" and "PB+H₂O" complexes (cf. Fig. 6), electron density differences (cf. Fig. 8), and electrostatic potential distributions practically coincide with those for a single cations.

## CONCLUSIONS

The O3LYP/6-31++G(d,p)/IEFPCM theory level reproduced the experimental spectra of PY and PB aqueous solutions quite accurately. According to calculations, the short-wavelength shoulders of these spectra are caused by vibronic transitions. The side groups significantly affect the set of vibronic transitions. The photoexcitation significantly changes the intensities of IR vibrations. The photoinduced decrease in the frequencies of these vibrations is small ($\approx$-50 cm$^{-1}$). The side groups of these xanthene dyes (aminodimethyl/aminodiethyl) strongly influence the vibrations of their chromophores. HOMOs cover the side groups of both dyes to a greater extent compared to LUMOs. At the same time, the configurations of both frontier orbitals around the chromophores are identical for PY and PB. The dipole moment of the dye molecules in the excited state turned out to be greater than in the ground state. In the ground state, the dipole moment of the PB is 2.5 times greater than that of the PY, and in the excited states, it is 1.7 times less. The transition moments of PY and PB are directed along the dye chromophores and are almost identical to each other. The excitations lead to a significant increase in electron densities at the C9 atoms and a decrease at C11 and C13 atoms. For PY, this charge shift is larger compared to PB which partly explains its higher absorption energy. Considering site-specific solute-solvent interactions in the form of an explicit assignment of water molecules that form strong hydrogen bonds with the dye cations led to a redshift of the entire spectrum by $\approx$3 nm for PY and fail of spectrum calculation for PB. For the "PB+H₂O" system a short-wavelength peak appeared, which was not observed in the experiment.

*References:*
1. Wright P. Xanth ene Dyes in Kirk-Othmer. *Encyclopedia of Chemical Technology*, 2000.
2. Kurnick N.B. Methyl green-pyronin; basis of selective staining of nucleic acids. *J. Gen. Physiol.*, 1950, vol. 33, pp. 243-264.
3. Darzynkiewicz Z., Kapuscinski J., Traganos F., Crissman H.A. Application of Pyronin Y(G) in Cytochemistry of Nucleic Acidsl. *Cytometry*, 1987, vol. 8, pp. 138-145.
4. Tomov T.C. Pyronin G as a fluorescent probe for quantitative determination of the membrane potential of mitochondria. *J. Biochem. Biophys. Methods*, 1986, vol.13, pp. 29-38.
5. Essawy A.A., Attia M.S. Novel application of pyronin Y fluorophore as high sensitive optical sensor of glucose in human serum. *Talanta*, 2013, vol. 107, p. 18-24.
6. Balraju P., Janu Y., Roy M.S., Sharma G.D. Dye Sensitized Solar Cell Based On Pyronin G Dye and TiO₂. *AIP Conf. Proc.*, 2008, vol. 1004, pp. 135-140.
7. Balraju P., Suresh P., Kumar M., Roy M.S., Sharma G.D. Effect of counter electrode, thickness and sintering temperature of TiO₂ electrode and TBP addition in electrolyte on photovoltaic performance of dye sensitized solar cell using pyronine G (PYR) dye. *J. Photochem. Photobiol. A*, 2009, vol. 206, pp. 53-63.

8. Muller W., Crothers D.M. Interactions of Heteroaromatic Compounds with Nucleic Acids. 1. The Influence of Heteroatoms and Polarizability on the Base Specificity of Intercalating Ligands. Eur. *J. Biochem.*, 1975, vol. 54, pp. 267-277.

9. Kapuscinski J. Interactions of Nucleic Acids with Fluorescent Dyes: Spectral Properties of Condensed Complexes. *J. Histochem. Cytochem.*, 1990, vol. 38, pp. 1323-1329.

10. Kapuscinski J., Darzynkiewicz Z. Interactions of Pyronin Y(G) With Nucleic Acids. *Cytometry*, 1987, vol. 8, pp. 129-137.

11. Salci A., Toprak M. Spectroscopic investigations on the binding of Pyronin Y to human serum albumin. *J. Biomol. Struct. Dyn.*, 2017, vol. 35, pp. 8-16.

12. Bordello J., Reija B., Al-Soufi W., Novo M. Host-Assisted Guest Self-Assembly: Enhancement of the Dimerization of Pyronines Y and B by γ-Cyclodextrin. *ChemPhysChem*, 2009, vol. 10, pp. 931-939.

13. Grauer Z., Grauer G.L., Avnir D., Yariv S. Metachromasy in Clay Minerals. Sorption of Pyronin Y by Montmorillonite and Laponite. *J. Chem. Soc., Faraday Trans.*, 1987, vol 83, pp. 1685-1701.

14. Senol A.M., Metin O., Acar M., Onganer Y., Meral K. The interaction of fluorescent Pyronin Y molecules with monodisperse silver nanoparticles in chloroform. *J. Mol. Structure*, 2016, vol. 1103, pp. 212-216.

15. Arik M., Onganer Y. Molecular excitons of Pyronin B and Pyronin Y in colloidal silica suspension. *Chem. Phys. Lett.*, 2003, vol. 375, pp. 126-133.

16. Senol A.M., Metin O., Onganer Y. A facile route for the preparation of silver nanoparticles-graphene oxide nanocomposites and their interactions with pyronin Y dye molecules. *Dyes Pigments*, 2019, vol. 162, pp. 926-933.

17. Gianneschi L.P., Kurucsev T. Derivation and Interpretation of the Spectra of Aggregates. Part 3.-Prediction Analytical Study of the Spectrum of Pyronine Y in Aqueous Solution. *J. Chem. Soc.*, 1974, vol. 70, pp. 1334-1342.

18. Gianneschi L.P., Cant A., Kurucsev T. Derivation and interpretation of the spectra of aggregates. *J. Chem. Soc.*, 1977, vol. 73, pp. 664-668.

19. Lee B.G., Kim K.J. Spectroscopic Characterization on the Aggregation Behavior of Pyronin G with Tetraphenylborate anion. *Anal. Sci. Technol.*, 1995, vol. 8, pp. 47-53.

20. Epelde-Elezcano N., Martinez-Martinez V., Duque-Redondo E., Temino I., Manzano H., López-Arbeloa I. Strategies for modulating the luminescence properties of pyronin Y dye-clay films: an experimental and theoretical study. *Phys. Chem. Chem. Phys.*, 2016, vol. 18, pp. 8730-8738.

21. Meral K., Yilmaz N., Kaya M., Tabak A., Onganer Y. The molecular aggregation of pyronin Y in natural bentonite clay suspension. *J. Luminesc.*, 2011, vol. 131, pp. 2121-2127.

22. Sinoforoglu M., Gur B., Arik M., Onganer Y., Meral K. Graphene oxide sheets as a template for dye assembly: graphene oxide sheets induce H-aggregates of pyronin (Y) dye. *RSC Adv.,* 2013, vol.3, pp. 11832-11838.

23. Fujiki K.O.N., Iwanaga C., Koizumi M. Some spectral studies of the aqueous solution of pyronine G. *Bull. Chem. Soc. Jpn*, 1962, vol. 35, pp. 185-193.

24. Arik M., Meral K., Onganer Y. Effect of surfactants on the aggregation of pyronin B and pyronin Y in aqueous solution. *J. Luminesc.*, 2009, vol.129, pp. 599-604.

25. Arik M., Kassa S.B., Onganer Y. Molecular aggregates of pyronin dyes with polyelectrolyte polystyrene sulfonate (PSS) in aqueous solution. *J. Photochem. Photobiol. A,* 2020, vol. 391, p. 112309.

26. Meral K., Erbil H.Y., Onganer Y. A spectroscopic study of water-soluble pyronin B and pyronin Y in Langmuir-Blodgett films mixed with stearic acid. *Appl. Surf. Sci.*, 2011, vol. 258, pp. 1605-1612.

27. Zhang X.-F., Zhang J., Lu X. The Fluorescence Properties of Three Rhodamine Dye Analogues: Acridine Red, Pyronin Y and Pyronin B. *J. Fluoresc.*, 2015, vol. 25, pp. 1151-1158.

28. Baraka M.E., Deumie M., Viallet P., Lampidis T.J. Fluorimetric studies of solutions of pyronin dyes: equilibrium constants in water and partition coefficients in organic-solvent-water systems. *J. Photochem. Photobiol. A*, 1991, vol. 56, pp. 295-311.

29. Celebi N., Arik M., Onganer Y. Analysis of fluorescence quenching of pyronin B and pyronin Y by molecular oxygen in aqueous solution. *J. Luminesc.*, 2007, vol. 126, pp. 103-108.

30. Rowe P.B. Spectrophotometry of dyes 1. Methyl green. 2. Pyronin. *Stain Tech.,* 1953, vol. 28, pp. 265-273.

31. Beser B.M., Onganer Y., Arik M. Photophysics and photodynamics of Pyronin Y in n-alcohols. *J. Luminesc.*, 2018, vol. 33, pp. 1394-1400.

32. Jakobsen P., Lyon H., Treppendahl S. Spectrophotometric characteristics and assay of pure pyronin Y. *Histochemistry*, 1984, vol 81, pp. 99-101.

33. Gur B., Meral K. The effect of poly (vinyl alcohol) on the photophysical properties of pyronin dyes in aqueous solution: A spectroscopic study. *Spectrochim. Acta A*, 2013 vol. 101, pp. 306-313.

34. Savarese M., Aliberti A., De Santo I., Battista E., Causa F., Netti P.A, Rega N. Fluorescence Lifetimes and Quantum Yields of Rhodamine Derivatives: New Insights from Theory and Experiment. *J. Phys. Chem. A*, 2012, vol. 116, pp. 7491-7497.

35. Zhou P. Why the lowest electronic excitations of rhodamines are overestimated by time-dependent density functional theory. *Int. J. Quantum Chem*, 2018, p. 25780.

36. Kulesza A.J., Titov E., Daly S., Wlodarczyk R., Megow J., Saalfrank P., Choi C.M., MacAleese L., Antoine R., Dugourd P. Excited States of Xanthene Analogues: Photofragmentation and Calculations by CC2 and Time-Dependent Density Functional Theory. *ChemPhysChem*, 2016, vol. 17, pp. 3129-3138.

37. Cossi M., Rega N., Scalmani G., Barone V. Energies, structures, and electronic properties of molecules in solution with the C-PCM solvation model. _J. Comput. Chem_., 2003, vol. 24, pp. 669-681.

38. Adamo C., Jacquemin D. The calculations of excited-state properties with Time-Dependent Density Functional Theory. _Chem. Soc. Rev._, 2013, vol. 42, pp. 845-856.

39. Charaf-Eddin A., Planchat A., Mennucci B., Adamo C., Jacquemin D. Choosing a Functional for Computing Absorption and Fluorescence Band Shapes with TD-DFT. _J. Chem. Theory Comput._, 2013, vol. 9 pp. 2749-2760.

40. Kostjukov V.V. Vibronic absorption spectra and excited states of acridine red dye in aqueous solution: TD-DFT/DFT study. _Z. fur Natur_. A, 2022, vol. 77, pp. 207-215.

41. Alia J.D., Flack J.A. Unspecified verticality of Franck-Condon transitions, absorption and emission spectra of cyanine dyes, and a classically inspired approximation. _RSC Adv.,_ 2020, vol. 10, pp. 43153-43167.

42. Tomasi J., Mennucci B., Cammi R. Quantum mechanical continuum solvation models. _Chem. Rev._, 2005, vol. 105, pp. 2999-3093.

43. Baiardi A., Bloino J., Barone V. General Time Dependent Approach to Vibronic Spectroscopy Including Franck-Condon, Herzberg-Teller, and Duschinsky Effects. _J. Chem. Theory Comput_., 2013, vol. 9, pp. 4097-4115.

44. Frisch M.J. et al. Gaussian 16, Revision C.01, Inc., Wallingford CT, 2016.

45. Condon E.U. Nuclear motions associated with electron transitions in diatomic molecules. _Phys. Rev._, 1928, vol. 32, pp. 858-872.

46. Scalmani G., Frisch M.J., Mennucci B., Tomasi J., Cammi R., Barone V. Geometries and properties of excited states in the gas phase and in solution: Theory and application of a time-dependent density functional theory polarizable continuum model. _J. Chem. Phys._, 2006, vol. 124, p. 94107.

47. Reed A.E., Curtiss L.A., Weinhold F. Intermolecular interactions from a natural bond orbital, donor-acceptor viewpoint. _Chem. Rev._, 1988, vol. 88, pp. 899-926.

48. Dennington R., Keith T.A., Millam J.M. GaussView, Version 6.1, Semichem Inc., Shawnee Mission KS, 2016.

49. Reichardt C. Solvatochromic Dyes as Solvent Polarity Indicators. _Chem. Rev._, 1994, vol. 94, pp. 2319-2358.

50. Zhao G.J., Han K.L. Effects of hydrogen bonding on tuning photochemistry: Concerted hydrogen-bond strengthening and weakening. _ChemPhysChem_, 2008, vol. 9, pp. 1842-1846.

51. Zhao G.-J., Han K.-L. Hydrogen Bonding in the Electronic Excited State. _Acc. Chem. Res_., 2012, vol. 45, pp. 404-413.

# ВОЗБУЖДЕНИЕ КРАСИТЕЛЕЙ ПИРОНИНА Y И ПИРОНИНА В В ВОДНОМ РАСТВОРЕ: СРАВНИТЕЛЬНЫЙ ТЕОРЕТИЧЕСКИЙ АНАЛИЗ

**Леонтьева С.В.**

Черноморское высшее военно-морское Ордена Красной Звезды училище имени П.С. Нахимова
_ул. Дыбенко 1а, г. Севастополь, 299028, РФ; e-mail: tezidi@gmail.com_

**Аннотация.** Чтобы выяснить влияние боковых групп на возбуждение ксантеновых красителей, пиронин Y (PY) и пиронин В (PB) были изучены методом DFT/TD-DFT. Результаты расчетов сравнивались между собой, а также с данными ранее исследованного красителя акридинового красного. Уровень теории O3LYP/6-31++G(d,p)/IEFPCM хорошо воспроизводил экспериментальные спектры водных растворов PY и PB. Согласно расчетам, коротковолновые плечи этих спектров обусловлены вибронными переходами. Боковые группы существенно влияют на набор вибронных переходов. Фотовозбуждение существенно изменяет интенсивность ИК-колебаний. Боковые группы этих ксантеновых красителей (аминодиметил/аминодиэтил) сильно влияют на колебания их хромофоров. HOMO покрывают боковые группы обоих красителей в большей степени, чем LUMO. Конфигурации обеих граничных орбиталей вокруг хромофоров идентичны для PY и PB. Дипольный момент молекулы красителя в возбужденном состоянии оказался больше, чем в основном состоянии. В основном состоянии дипольный момент PB в 2,5 раза больше, чем у PY, а в возбужденных состояниях – в 1,7 раза меньше. Моменты перехода PY и PB практически идентичны друг другу. Проведен учет сайт-специфических взаимодействий растворенное вещество-растворитель в виде явного отнесения молекул воды, образующих прочные водородные связи с катионами красителей.

_**Ключевые слова:**_ _TD-DFT, вибронные переходы, водный раствор, пиронин Y, пиронин Б, спектр поглощения._